Simplified cascade multiphase DC-DC boost power converters for high voltage-gain and low-ripple applications

Pekik Argo Dahono
School of Electrical Engineering and Informatics, Institute of Technology Bandung, Indonesia

Article Info

ABSTRACT

This paper proposes two new simplified cascade multiphase DC-DC boost power converters with high voltage-gain and low ripple. All simplifications reduce the number of active switching devices from *2N* into *N*, where *N* is the phase number. The first simplification reduces the number of inductors from *2N* into *N+1* and increases the number of diodes from *2N* into (*2N+1*). The second simplification reduces the number of inductors from *2N* into *N+1* and increases the number of diodes from *2N* into (*3N+1*). The second simplification needs inductors with smaller current rating than the first simplification. The expressions of output voltage as a function of load current are derived by taking into account the voltage drops across the inductors and switching power devices. Simulated and experimental results are included to show the basic performance of the proposed cascade multiphase DC-DC boost power converters.

Corresponding Author:

Pekik Argo Dahono
School of Electrical Engineering and Informatics
Institute of Technology Bandung
Jl. Ganesa No. 10, Bandung 40132, Indonesia
Email: padahono@ieee.org

1. INTRODUCTION

A very high-gain step-up DC-DC power converter is commonly used in photovoltaic (PV) and fuel-cell power generation systems. In a microconverter, for example, the output voltage of each PV module (about 36-42 Vdc) has to be increased directly into 400 Vdc. By using a microconverter, each module has own MPPT (maximum power point tracking) controller to minimize the effects of shading. Depending on the number of stacks, the dc output voltage of fuel cells is also very low between 12 and 60 Vdc [1]. In addition to high voltage-gain, high efficiency and minimum input and output ripples are desirable. High voltage-gain capabilities are usually obtained by cascading several two or more DC-DC boost power converters. Minimum input and output ripples can be obtained by using multiphasing or interleaving technique. A very low input current ripple is necessary to ensure the long life of PV modules and fuel cells. High efficiency can be obtained by using soft switching techniques and eliminating the isolation transformer.

Cascade connection of several DC-DC boost power converters to increase the reachable voltage-gain were discussed in [2]-[4]. These works have shown that different power converters can be cascaded to achieve certain properties. Simplification to reduce the number of active switching devices was proposed in [5]-[10]. These works are limited to single-phase DC-DC power converters. Cascade connection of several multiphase DC-DC boost power converters to reduce the input current ripple were also presented in [11]-[12]. By cascading several multiphase DC-DC boost power converters, a zero input current ripple can also be achieved as well as very high voltage-gain. Cascading several multiphase DC-DC boost power converters, however, needs a large number of inductors and active switching devices. As far as the author is aware, how

to reduce the component count of cascade multiphase DC-DC boost power converters has not been proposed. Another method to increase the voltage gain is by using a dual boost topology [13]-[15]. In this case, the inputs of two boost converters are connected in parallel and the outputs are in series. The main disadvantage of this approach is that there is no common point between the input and output terminals.

This paper proposes two new simplified cascade multiphase DC-DC boost power converters with very high voltage-gain and low input current ripple. All simplifications reduce the number of active switching power devices from *2N* into *N*, where *N* is the phase number. The first simplification reduces the number of inductors from *2N* into *(N+1)* and increases the number of diodes from *2N* into (2N+1). The second simplification reduces the number of inductors from *2N* into *N+1* and increases the number of diodes from *2N* into *(3N+1)*. The expressions of output voltage as a function of load current are derived by taking into account the voltage drops across the inductors and switching power devices. A comparative evaluation among cascade multiphase DC-DC boost power converters is provided. Simulated and experimental results are included to show the basic performance of the proposed cascade multiphase DC-DC boost power converters.

The rest of the paper is organized as follows. Section two discuss the conventional cascade single-phase and multiphase DC-DC boost converters. Section three discuss the derivation of two new simplified cascade multiphase DC-DC boost converters. Section four discuss the performance comparison among the cascade multiphase DC-DC boost power converters. Section five discuss the experimental results and Section six is the conclusion.

2. CONVENTIONAL CASCADE MULTIPHASE DC-DC POWER CONVERTERS

Conventional cascade multiphase DC-DC boost power converters are first discussed here. Simplification of these converters are discussed in the next section. Figure 1 shows the cascade connection of single-phase DC-DC boost power converters and the simplified version. By using the cascade connection as shown in Figure 1(a), the voltage-gain under continuous inductor current mode is (1)

$$\frac{V_o}{E_d} = \frac{1}{(1-\alpha_1)(1-\alpha_2)}$$

(1)

where α_1 and α_2 are the duty cycles of the front and rear converter switching power devices, respectively. The maximum value of duty cycle is unity.

Simplification method of cascaded connection of two DC-DC boost converter in Figure 1(a) into the one as shown in Figure 1(b) was discussed in [5]-[10]. As it is shown in Figure 1(b), the simplified cascade single-phase DC-DC boost power converter needs just one active switching power devices but the number of diodes is increased into three. Under continuous inductor current mode, the voltage gain is (2)

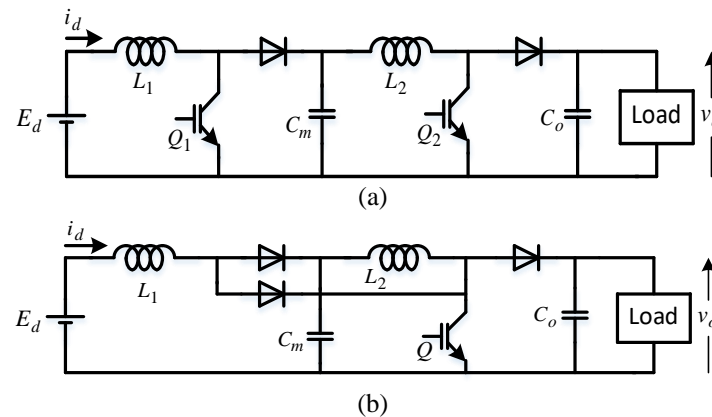$$\frac{V_o}{E_d} = \frac{1}{(1-\alpha)^2}$$

(2)

Figure 1. Cascade connection of single-phase DC-DC boost converters, (a) cascade connection of single-phase DC-DC boost converters, (b) simplified cascade single-phase DC-DC boost converters

Thus, the voltage-gain of simplified cascade single-phase DC-DC boost converter has a quadratic characteristic. Analysis and control this quadratic converter have been proposed in [16]-[18]. For the same duty cycle, the original and simplified cascade single-phase DC-DC boost power converters have a voltage-gain that is higher than just a single-phase DC-DC boost power converter. This cascade connection can be extended to more than two DC-DC boost power converters. Though cascading several DC-DC boost converters can solve the voltage-gain problem, the input and output ripples are still high. In single-phase DC-DC boost converter, the ripples are usually reduced by increasing the switching frequency and/or the filter size.

It has been shown in the literature that multiphasing or interleaving is an effective way to reduce the input and output current ripples without using a high switching frequency nor a large filter [19]-[21]. Similarly, in order to reduce the input and output ripples and to obtain a high voltage-gain, two or more multiphase DC-DC boost power converters can be cascaded as shown in Figure 2. By using this cascade connection, the voltage-gain is the same as given by (1). The phase numbers of front and rear multiphase DC-DC boost power converters in Figure 2 do not have to be the same. If the duty cycle of the first stage converter is selected constant at certain values, the input current ripple can be almost equal to zero [20]. In this case, the output voltage control is delegated into the rear stage DC-DC boost power converter. The switching frequencies of the front and rear stages of DC-DC boost power converters do not have to be the same and can be optimized to maximize the efficiency. Though the input output ripples are reduced significantly by cascading several multiphase DC-DC boost power converters, the numbers of inductors and switching devices are significantly increased.

The simplified single-phase cascade DC-DC power converter in Figure 1(b) can also be extended into the multiphase one as shown in Figure 3. Similar to conventional multiphase DC-DC boost converters, the active switching devices are gated by identical carrier signals with phase difference of $2\pi/N$. The voltage-gain of this converter is the same as given by (2). Though the number of active switching power devices is reduced from $2N$ into N, the number of diodes is increased from $2N$ into $3N$ and the number of electrolytic capacitors is increased from two into $N+1$.
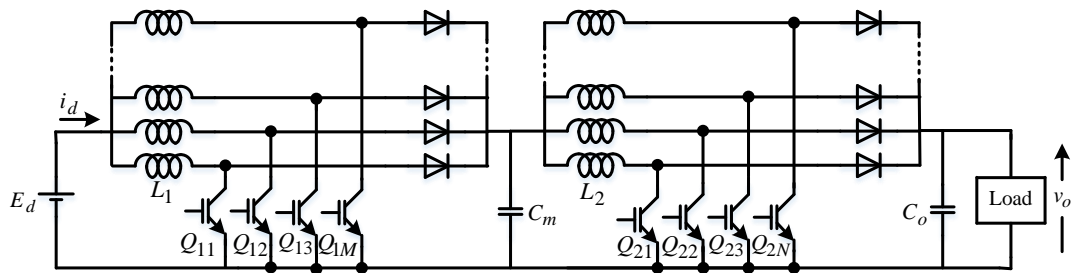

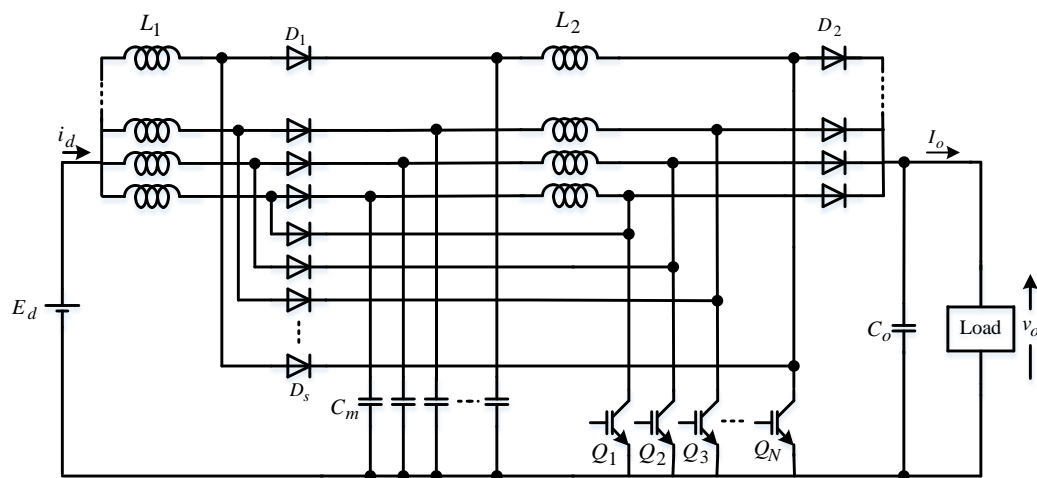Figure 2. Cascade connection of multiphase DC-DC boost converters

Figure 3. Simplified cascade multiphase DC-DC boost converters

3.   SIMPLIFIED CASCADE MULTIPHASE DC-DC POWER CONVERTERS
3.1. First simplification

As the duty cycles of transistors in Figure 3 are equals, the average voltages across capacitors Cm are equal. As the voltages are equal, the capacitors C_m can be connected directly in parallel. If these capacitors C_m are connected in parallel, the inductors L_1 and diodes D_1 will also be in parallel. Thus, the converter can be simplified into the first simplified cascade multiphase DC-DC boost converter as shown in Figure 4.

In the new converter of Figure 4, the number of inductors is reduced from *2N* into *(N+1)*. The active switching power devices are reduced from *2N* into *N*. The number of diodes, however, is increased from *2N* into *(2N+1)* compared to the one in Figure 2. Similar to conventional multiphase DC-DC boost converter, the same gating strategy as conventional multiphase dc- dc boost converter is used here. Under continuous inductor current mode, the voltage-gain is (3)

$$\frac{V_o}{E_d} = \frac{1}{(1 - N\alpha)(1 - \alpha)}$$

(3)

where the maximum value of duty cycle is *1/N*. If the duty cycle is more than *1/N*, the input voltage will be short-circuited through the active switching devices.

As the maximum duty cycle is reduced, the phase number can't be increased too high. In the DC-DC power converter of Figure 4, the number of inductors of the front stage DC-DC boost power converter has been reduced from *N* into one. Moreover, the required inductance to ensure continuous conduction mode is also *1/N* smaller compared to the original one. In this case, however, the required current rating of the inductor will be large as the front DC-DC boost converter works at the low voltage side.

Figure 5 shows simulated result for the converter in Figure 4 with phase number of two. The converter was simulated by using PSIM. In the simulation, it is assumed that dc voltage source is 12 V. The inductors L_1 and L_2 are equal with the inductance of one mH. The capacitors C_m and C_o are equal with the capacitance of 200 uF. The switching frequency is 5 kHz. In the simulation, it is also assumed that all components are ideal components. The load is assumed as a constant resistance of 100 Ohm. Figure 5 shows that the ripple frequency of the input current is two times of the switching device frequency. The duty cycle of 0.41 is used to obtain an output voltage of 120 Vdc. As the input side inductor current ripple is *N* times of the switching device frequency, the size of the inductor can be reduced significantly.
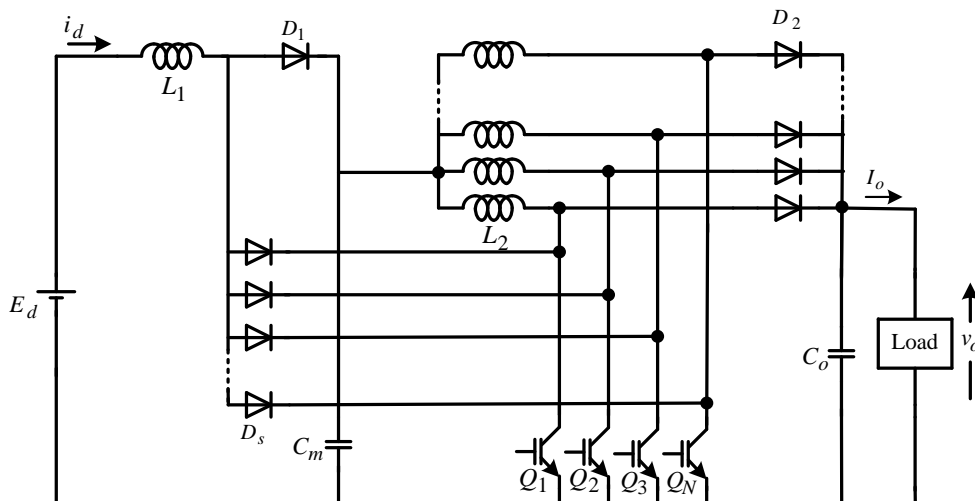

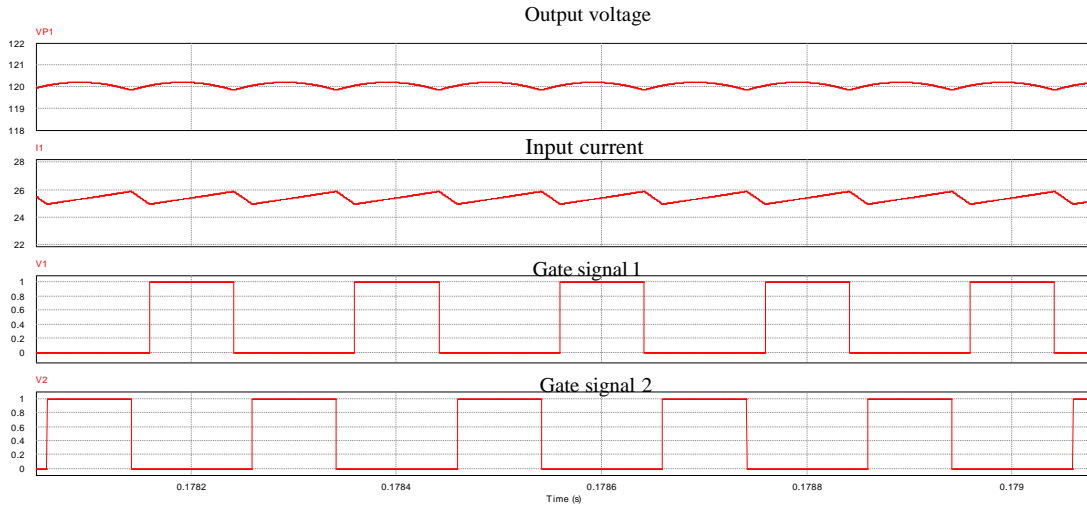Figure 4. First simplified cascade multiphase DC-DC boost converter

Figure 5. Simulated result of first simplified cascade two-phase DC-DC boost converter

3.2. Second simplification

As it was previously mentioned, the average voltages across capacitors C_m are equal when the duty cycles of switching devices are equal. Thus, the inductors L_2 and D_2 will be connected in parallel. As connected in parallel, N inductors L_2 and diodes D_2 can be replaced into just single inductor L_2 and single diode D_2 as shown in Figure 6. In this case, however, additional series diodes are required to prevent currents from inductors L_1 are flowing through the undesired transistors. The numbers of inductors and active switching power devices are also reduced as in the case of Figure 4. The number of diodes, however, is increased from *2N* into *(3N+1)*. In this case, however, the single inductor is working on the high voltage side and, therefore, the required current rating is small. Moreover, the ripple frequency of the current through the second stage inductor is N times of the switching frequency and, therefore, the required inductance is small. The voltage-gain is still the same as given by (3).

Figure 7 shows simulated result for the converter in Figure 6 with phase number of two. In the simulation, the system data is the same as the used in Figure 5. Figure 7 shows that the ripple frequency of the input current is two times of the switching device frequency and also two times of the input side inductor current ripple. The duty cycle of 0.41 is used to obtain an output voltage of 120 Vdc.

It has been mentioned that the maximum duty cycle will be significantly reduced when the phase number is high. In order to solve this problem, an even phase number can be obtained by paralleling several simplified cascade two-phase DC-DC boost converters. Figure 8 shows simplified cascade four-phase DC-DC boost converter that is obtained by paralleling two simplified cascade two-phase DC-DC boost converters. The carrier signals for the first and second simplified cascade two-phase DC-DC boost converters are shifted by 90o in order to obtain four phase DC-DC boost converter characteristic. The voltage gain of this converter is (4)

$$\frac{V_o}{E_d} = \frac{1}{(1-2\alpha)(1-\alpha)} \tag{4}$$

By using this method, the maximum duty cycle is half instead of one fourth.

The proposed simplification approach can also be applied to cascade connection of more than two multiphase DC-DC boost power converters. Figure 9 shows the extension of Figure 4 when the number of stages is three. In this case, the voltage gain under continuous inductor current mode is (5)

$$\frac{V_o}{E_d} = \frac{1}{(1-N\alpha)^2(1-\alpha)} \tag{5}$$

Extension of the scheme in Figure 6 into more than two stages will need more inductors than the extension of Figure 4. Thus, extension of Figure 4 is preferred when the number of stages is more than two.
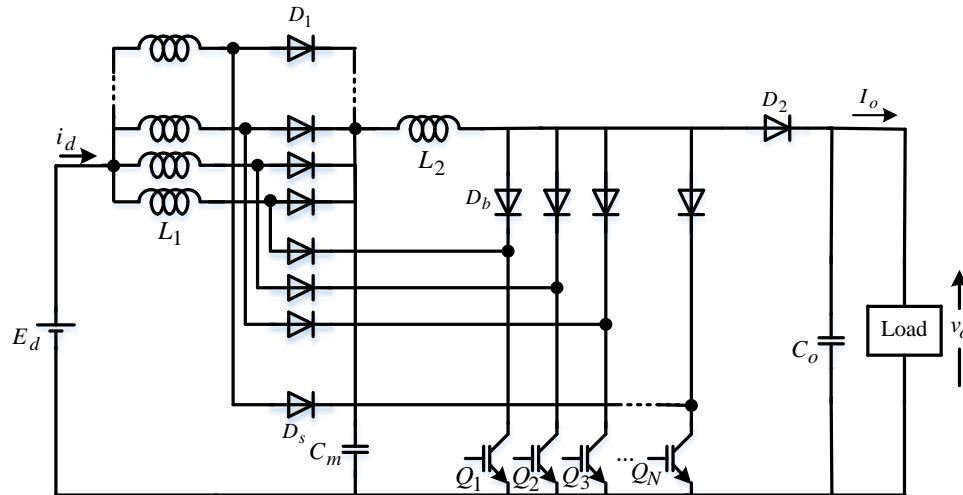
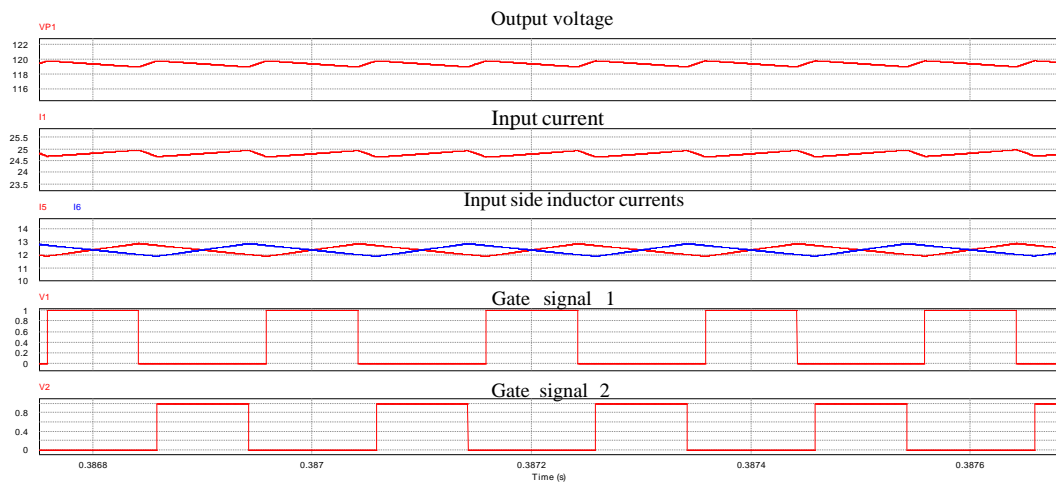Figure 6. Second simplified cascade multiphase DC-DC boost converter

Figure 7. Simulated result of second simplified cascade two-phase DC-DC boost converter
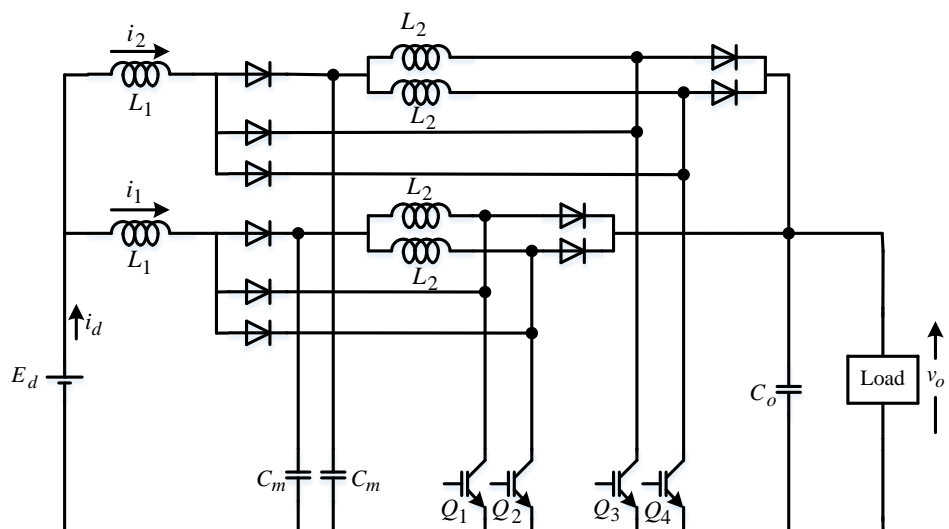

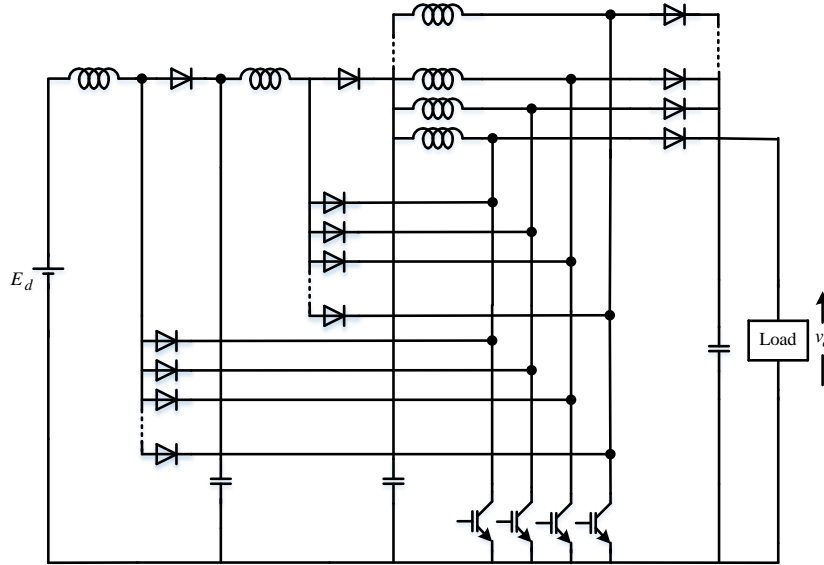Figure 8. Simplified cascade four-phase DC-DC boost converter

Figure 9. Simplified three-stages cascade multiphase DC-DC boost converter

4.   COMPARATIVE EVALUATION
4.1. Output voltage analysis

The output voltage expressions (1)-(3) have been derived by assuming that the voltage drops across the inductors and switching power devices are negligible. If these voltage drops are neglected, the output voltage can be increased up to infinitely. In practices, the voltage drops across the inductors and switching power devices will limit the maximum output voltage that can be achieved.

The expressions of output voltage by taking into account the voltage drops across the inductors and switching power devices can be obtained by using state-space averaging technique [22]. The obtained results are shown in Table 1. These expressions are valid under continuous inductor current mode. All capacitors were assumed as ideal capacitors with no parasitic components. All inductors have the same resistances of R_L. All active switching power devices and diodes are assumed as identical. The voltage drops across the switching devices during conduction mode are represented by a constant component plus a resistive component. V_Q and V_D are constant components and R_Q and R_D are resistive components of voltage drops across the transistors and diodes, respectively.

Table 1. Output voltage expressions

Figure	Output voltage expression
2	$\bar{v}_o = \dfrac{E_d}{(1-\alpha)^2} - \dfrac{\left[V_Q\alpha + V_D(1-\alpha)\right](2-\alpha)}{(1-\alpha)^2} - \dfrac{\left[R_L + R_Q\alpha + R_D(1-\alpha)\right]\left(2-2\alpha+\alpha^2\right)}{N(1-\alpha)^4}I_o$
3	$\bar{v}_o = \dfrac{E_d}{(1-\alpha)^2} - \dfrac{V_Q\alpha(2-\alpha)+V_D\left(2-2\alpha+\alpha^2\right)}{(1-\alpha)^2} - \dfrac{R_Q\alpha(2-\alpha)^2}{N(1-\alpha)^4}I_o$ $- \dfrac{R_L\left(2-2\alpha+\alpha^2\right)}{N(1-\alpha)^4}I_o - \dfrac{R_D\left(2-3\alpha+3\alpha^2-\alpha^3\right)}{N(1-\alpha)^4}I_o$
4	$\bar{v}_o = \dfrac{E_d}{(1-N\alpha)(1-\alpha)} - \dfrac{V_Q\alpha[1+N-N\alpha]}{(1-N\alpha)(1-\alpha)} - \dfrac{V_D\left(2-\alpha-N\alpha+N\alpha^2\right)}{(1-N\alpha)(1-\alpha)} - \dfrac{R_L\left[N+(1-N\alpha)^2\right]}{N(1-N\alpha)^2(1-\alpha)^2}I_o$ $- \dfrac{R_D\left[N+(1-\alpha)(1-N\alpha)^2\right]}{N(1-N\alpha)^2(1-\alpha)^2}I_o - \dfrac{R_Q\alpha\left(1+N+2N^2-2N\alpha-N^2\alpha-N^3\alpha+N^2\alpha^2\right)}{N(1-\alpha)^2(1-N\alpha)^2}I_o$
6	$\bar{v}_o = \dfrac{E_d}{(1-N\alpha)(1-\alpha)} - \dfrac{V_Q\alpha[1+N(1-\alpha)]+V_D(2-\alpha)}{(1-N\alpha)(1-\alpha)} - \dfrac{R_L\left[1+N(1-\alpha)^2\right]}{N(1-N\alpha)^2(1-\alpha)^2}I_o$ $- \dfrac{R_D\left[1+N(1-\alpha)^2\right]}{N(1-N\alpha)^2(1-\alpha)^2}I_o - \dfrac{R_Q\alpha\left[1+N+2N^2-N\alpha-3N^2\alpha+N^2\alpha^2\right]}{N(1-N\alpha)^2(1-\alpha)^2}I_o$

Output voltage expressions in Table 1 for the first and second simplified converters are plotted as shown in Figure 10. It is assumed that the active switching devices are MOSFETS (IRFP240). According to the data sheet, the resistance of IRFP240 is 18 mΩ. All diodes are RHRP3060 with a constant voltage drop of 0.9 V and a resistance of 16 mΩ. Inductor resistances are assumed equal to 50 mΩ. It is assumed that the dc input voltage is constant at 12 Vdc. The no load voltages are assumed the same at 120 Vdc. This figure shows that the output voltages of first and second simplified cascade multiphase DC-DC boost converters are higher than the ones in Figures 2 and 3. The voltage drops of first simplified converter are almost not changed when the phase number is increased. On the other hand, the voltage drops of the second simplified converter are increased when the phase number is increased. In practices, the inductors of the front and rear stages of the simplified converters will be different and can be optimized to reduce the voltage drops.
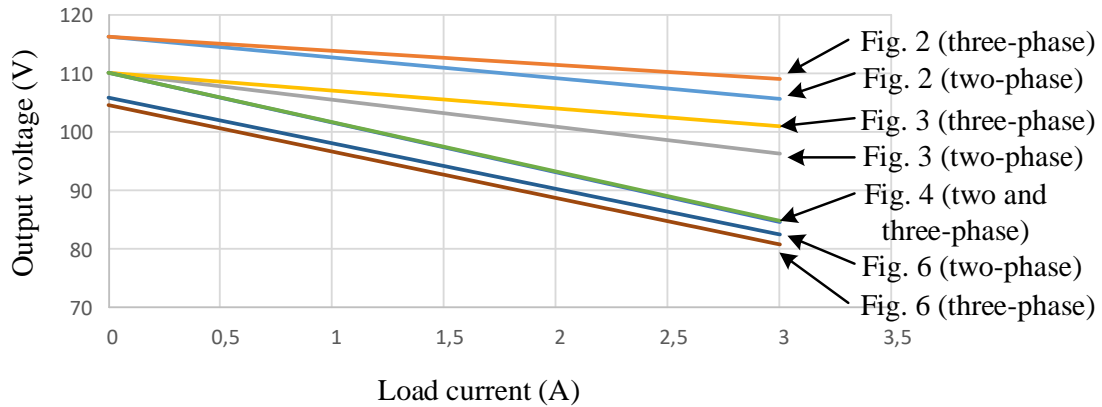

Figure 10. Output voltage as a function of load current

4.2. Conduction losses

The output power of the DC-DC power converter is (6)

$$P_o = \bar{v}_o I_o \tag{6}$$

By using the output voltage expression in Table 1 and (3), the output power of the simplified cascade multiphase DC-DC boost power converter, Figure 3 for example, is (7)

$$P_o = \frac{E_d}{(1-\alpha)^2} I_o - \frac{V_Q \alpha(2-\alpha) + V_D \left(2 - 2\alpha + \alpha^2\right)}{(1-\alpha)^2} I_o$$
$$- \frac{R_Q \alpha(2-\alpha)^2 + R_D \left(2 - 3\alpha + 3\alpha^2 - \alpha^3\right) + R_L \left(2 - 2\alpha + \alpha^2\right)}{N(1-\alpha)^4} I_o^2 \tag{7}$$

The input current of the DC-DC power converter is (8)

$$\bar{i}_d = \frac{I_o}{(1-\alpha)^2} \tag{8}$$

Substituting (8) into (7), the (9) is obtained

$$P_o = E_d \bar{i}_d - \frac{V_Q \alpha(2-\alpha) + V_D \left(2 - 2\alpha + \alpha^2\right)}{(1-\alpha)^2} I_o$$
$$- \frac{R_Q \alpha(2-\alpha)^2 + R_D \left(2 - 3\alpha + 3\alpha^2 - \alpha^3\right) + R_L \left(2 - 2\alpha + \alpha^2\right)}{N(1-\alpha)^4} I_o^2 \tag{9}$$

The power loss in the converter is (10)

$$P_{loss} = P_i - P_d \tag{10}$$

The converter input power is (11)

$$P_i = E_d \bar{i}_d \tag{11}$$

By using (8)-(11), the (12) is obtained:

$$P_{loss} = \frac{V_Q \alpha (2-\alpha) + V_D \left(2 - 2\alpha + \alpha^2\right)}{(1-\alpha)^2} I_o$$

$$+ \frac{R_Q \alpha (2-\alpha)^2 + R_D \left(2 - 3\alpha + 3\alpha^2 - \alpha^3\right) + R_L \left(2 - 2\alpha + \alpha^2\right)}{N(1-\alpha)^4} I_o^2 \tag{12}$$

Equation (12) shows that the voltage drops across the switching devices and inductors can be used to estimate the conduction losses. As the voltage drops in the simplified converters are bigger than the original ones, the conduction losses are also bigger. As it has been mentioned before, the inductor L_1 in Figure 4 or the inductor L_2 in Figure 6 can be made smaller and, therefore, the conduction losses can be smaller.

4.3. Switching losses

The switching losses are proportional to the operating voltage and current [23]-[27]. In general, the switching losses in a transistor can be written as (13)

$$P_{sw} = Kf_s VI \tag{13}$$

where K is a constant that depends on the device characteristics, f_s is switching frequency, V is the device operating voltage, and I is the device current. By using a simple analysis, the expressions of switching losses of cascaded multiphase boost converters are given in Table 2. These expressions are plotted in Figure 11.

Figure 11 shows that the first simplified converter has higher switching losses than the others. Though the second simplified converter has higher conduction losses than the first one, the switching losses are smaller. In general, the proposed multiphase DC-DC boost converters have a smaller count number of components but at the expense of higher losses. The losses can be reduced if modern wide bandgap power devices are used [26], [27].

As the conduction and switching losses are high compared to conventional cascade multiphase DC-DC boost power converters, the proposed simplified cascade multiphase DC-DC power converters are suitable only for low-power applications such as microconverters. Though the losses are high, the proposed converters need a smaller count of inductors and capacitors. In some cases, the inductors and capacitors take more volume than the semiconductors and the associated controllers.

Table 2. Switching losses

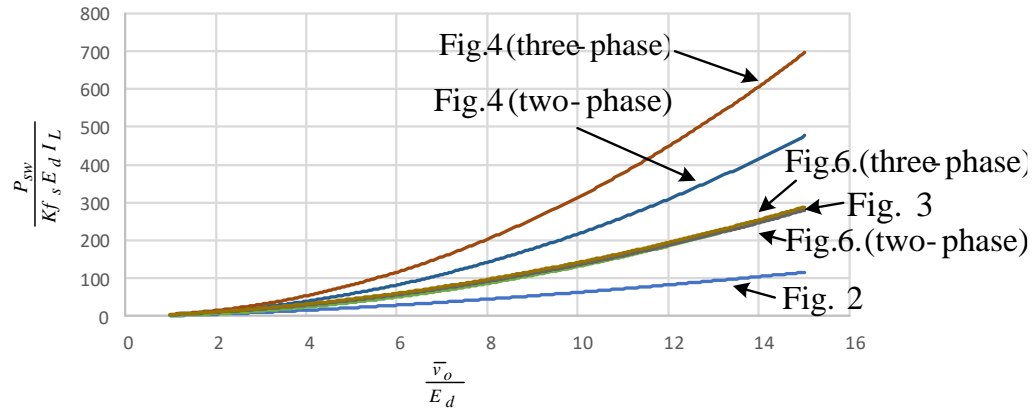| Figure	Output voltage expression
2	$P_{sw} = 2Kf_s E_d \dfrac{I_L}{(1-\alpha)^3}$
3	$P_{sw} = \dfrac{Kf_s E_d I_L}{(1-\alpha)^4}(2-\alpha)$
4	$P_{sw} = \dfrac{Kf_s E_d I_L}{(1-\alpha)^2 (1-N\alpha)^2}\left[(1-N\alpha) + N\right]$
6	$P_{sw} = \dfrac{Kf_s E_d I_L}{(1-\alpha)^2 (1-N\alpha)^2}\left[N(1-N\alpha) + 1\right]$

Figure 11. Switching losses

5. EXPERIMENTAL RESULTS

A small simplified cascade multiphase DC-DC boost converter system with the scheme as shown in Figure 4 was constructed. The phase number N is two. All inductors have identical inductance of 5.1 mH and resistance of 0.3 Ohm. The active switching devices were implemented by using power MOSFETs (IRFP240) with resistance of 18 mΩ. A TLP250 gate driver was used to drive the MOSFET. All diodes (RHRP3060) have constant voltage drop of 0.9 V and resistance of 16 mΩ. The switching frequency was maintained constant at 10 kHz during the experiment. The dc input voltage is also maintained constant at 12 Vdc. The load is a variable resistance. No attempts have been done to optimize the converter performance by selecting better inductors and semiconductor devices.

Figure 12 shows the input current and gate signal waveforms of simplified cascade two-phase DC-DC boost converter. It can be seen that the input current ripple frequency is twice the gate signal frequency. In this figure, O is the zero point of current and G is the zero point of gate signal.

Figure 13 shows the input current ripple as a function of voltage-gain when the load resistance is fixed at 100 Ohm. For comparison, the result of simplified cascade single-phase DC-DC boost converter is also shown. In this figure, the triangle and square marks are experimental results and lines are calculated results. The current ripples were calculated by a method as described in [20]. It can be seen that the input current ripple of simplified cascade two-phase DC-DC boost converter is much smaller than the single phase one. Discrepancies between calculated and measured results are possibly due to the nonlinearity of iron core inductors. The ripple can be reduced further by increasing the phase number.
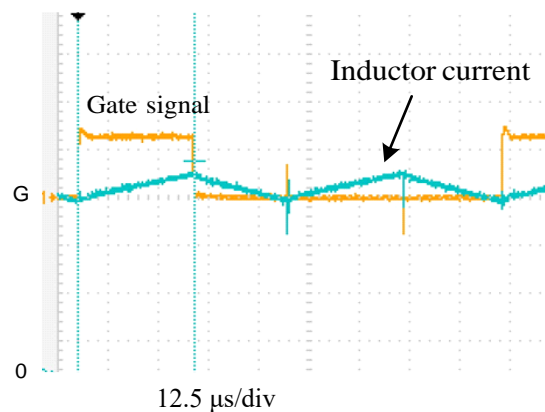

Figure 12. Input current (2 A/div) and gate signal (5 V/div) waveforms

Figure 14 shows the experimental and calculated results of voltage-gain as a function of duty cycle when the load resistance is fixed at 100 Ohm. Though the resistance of inductors is large, a voltage-gain

more than eight can be reached easily by the proposed converter. Figure 14 also shows that the experimental results are close to the calculated ones. Higher voltage gain can be obtained by using number of stages more than two.

Figure 15 shows the output voltage as a function of the output current. The output current is changed by changing the load resistance while maintaining the duty cycle constant. In this figure, cross mark is experimental results and line is calculated results. Based on Figures 14 and 15, validity of the derived expression as shown in Table 1 can be appreciated. Discrepancies between calculated and measured results are possibly due to the inaccuracy of inductor resistances.
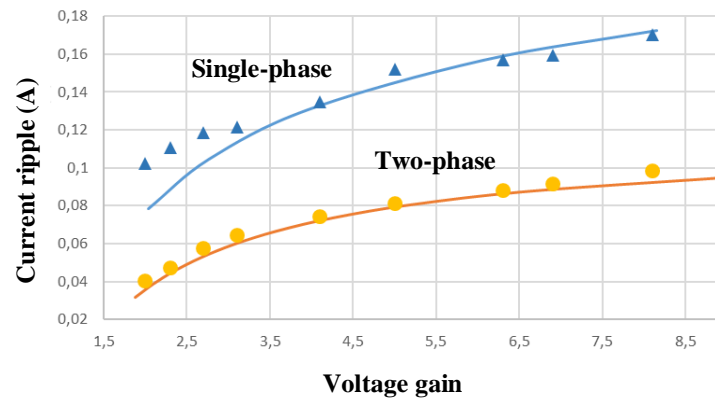
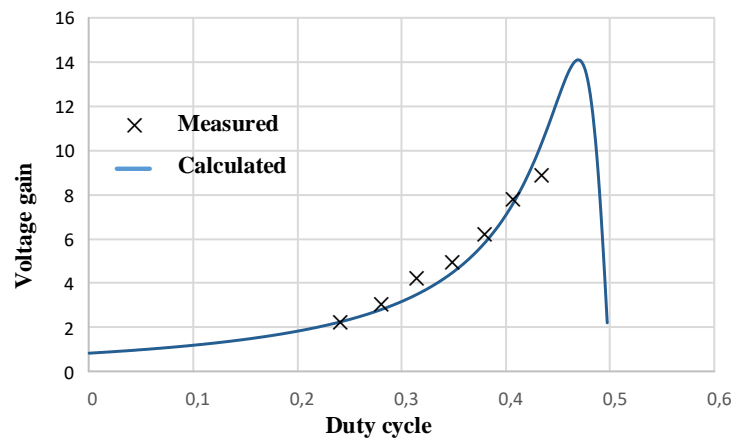Figure 13. Input current ripple as a function of voltage-gain

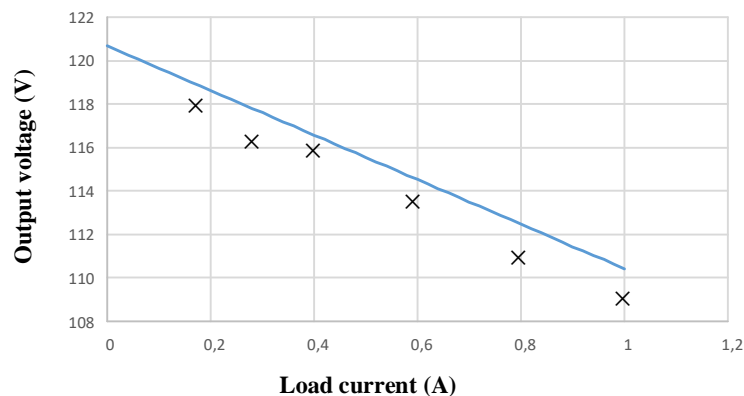Figure 14. Voltage gain as a function of duty cycle

Figure 15. Output voltage as a function of load current

6. CONCLUSION

Two simplified cascade multiphase DC-DC boost power converters for high voltage-gain and low-ripple applications have been proposed in this paper. By using the proposed converters, high voltage-gain and small input and output ripples, can be obtained with a smaller number of active switching power devices. Voltage-gain comparison among the proposed converters is shown in this paper. A method is presented to solve the problem of limited duty cycle range when the phase number is high. The proposed method can also be extended to cascade connection more than two multiphase DC-DC boost converters. Output voltage analysis that is useful to estimate the conduction losses is also presented. As the power losses are higher than the conventional cascade multiphase DC-DC boost power converters, the proposed converters are suitable for low-power applications such as microconverters. Experimental results that showing the basic performance have been included. Selection of the optimal components for the proposed converters is under investigation.

REFERENCES

[1] H. Liu *et al.*, "Short-term prognostics of PEM fuel cells: A comparative and improvement study," *IEEE Trans. Ind. Electron*, vol. 66, no. 8, pp. 6077–6086, Aug. 2019.

[2] H. Matsuo and K. Harada, "The cascade connection of switching regulators," *IEEE Trans. Ind. Appl*, vol. 12, no. 2, pp. 192–198, 1976.

[3] F. L. Tofoli *et al.*, "Survey on nonisolated high-voltage step-up DC-DC topologies based on the boost converter," *IET Power Electron*, vol. 8, no. 10, pp. 2044–2057, 2015.

[4] M. Forouzesh *et al.*, "Step-up DC-DC converters: A comprehensive review of voltage boosting techniques, topologies, and applications," *IEEE Trans. Power Electron*, vol. 32, no. 12, pp. 9143–9178, 2017.

[5] R. D. Middlebrook, "Transformerless dc-to-dc converters with large conversion ratios," *IEEE Trans. Power Electronics*, vol. 3, no. 4, pp. 484–488, 1988.

[6] D Maksimovic and S. Cuk, "Switching converters with wide dc conversion range," *IEEE Trans. Power Electron*, vol. 6, no. 1, pp. 151–157, 1991.

[7] F. L. Luo and Y. Ye, "Positive output cascade boost converters," *IEE Electr. Power Appl*, vol. 151, no. 5, pp. 590–606, 2004.

[8] R. Lorea-Palomo and J. A. Morales-Saldana, "Family of quadratic step-up DC-DC converters based on non cascading structures," *IET Power Electron*, vol. 8, no. 5, pp. 793–801, 2015.

[9] M. I. Nejad *et al.*, "New cascade boost converter with reduced losses," *IET Power Electron*, vol. 9, no. 6, pp. 1213–1219, 2016.

[10] J. Chen *et al.*, "Cascaded high voltage conversion ratio bidirectional nonisolated DC-DC converter with variable switching frequency," *IEEE Trans. Power Electron*, vol. 33, no. 2, pp. 1399–1409, 2018.

[11] R. Hosoki, S. Kinjo, and H. Koizumi, "Ripple free operation of two-stage boost type DC-DC converter," *Proc. IEEE Industrial Electronics Conference*, 2015, pp. 577–582.

[12] S. Hayano and N. Hoshi, "Efficiency characteristic of cascaded multistage boost converter," *Proc. IEEE Industrial Electronics Conference*, 2016, pp. 1324–1329.

[13] O. Lopez-Santos *et al.*, "Steady-State analysis of inductor conduction modes in the quadratic boost converter," *IEEE Trans. Power Electron*, vol. 32, no. 5, pp. 2253–2264, 2017.

[14] J. A. Morales-Saldana *et al.*, "Multiloop controller design for a quadratic converter," *IET Electr. Power Appl*, vol. 1, no. 3, pp. 362–367, 2007.

[15] C. Y. Chan, "Investigation of voltage-mode controller for cascade boost converter," *IET Power Electron*, vol. 7, no. 8, pp. 2060–2068, 2014.

[16] S. Choi *et al.*, "Analysis, design and experimental results of a floating-output interleaved-input boost-derived DC-DC high-gain transformerless converter," *IET Power Electron*, vol. 4, no. 1, pp. 168–180, 2011.

[17] M. Kabalo *et al.*, "Experimental validation of high-voltage-ratio low-input-current-ripple converters for hybrid fuel cell supercapacitor systems," *IEEE Trans. Vehicular Tech*, vol. 61, no. 8, pp. 3430–3440, Oct. 2012.

[18] P. A. Dahono, "Derivation of high voltage-gain step-up DC-DC power converters," *International Journal of Electrical Engineering and Informatics*, vol. 11, no. 2, pp. 236–251, Jun. 2019.

[19] R. Giral, L. Martinez-Salamero, and S. Singer, "Interleaved Converter Operation Based on CMC," *Trans Power Electron*, vol. 14, no. 4, pp. 643–652, Jul. 1999.

[20] P. A. Dahono *et al.*, "Output Ripple Analysis of Multiphase DC-DC Converters," *Proc. IEEE Power Electronics, Drives, and Systems Conference*, 1999, pp. 626–631.

[21] P. W. Lee *et al.*, "Steady-State Analysis of an Interleaved Boost Converter with Coupled Inductors," *IEEE Trans. Ind. Electron*, vol. 47, no. 4, pp 787–795, Aug. 2000.

[22] R. D. Middlebrook and S. Cuk, "A general unified approach to modelling switching-converters power stages," *Proc. IEEE Power Electronics Specialist Conference*, 1976, pp. 18–34.

[23] J. H. Rockot, "Losses in High-Power Bipolar Transistors," *IEEE Trans. Power Electron*, vol. 2, no. 1, pp. 72–80, Jan. 1987.

[24] P. A. Dahono, Y. Sato, and T. Kataoka, "Analysis of Switching and Conduction Losses in Hysteresis Current Controlled Inverters," *IEE Japan Trans. Industry Appl*, vol. 113-D, no. 10, pp. 1216–1225, 1993.

[25] F. Blaabjerg, U. Jaeger, and J. K. Padersen, "Power Losses in PWM-VSI Inverter Using NPT or PT IGBT Devices," *IEEE Trans. Power Electron*, vol. 10, no. 3, pp. 358–367, May 1995.

[26] F. Xue *et al*., "Loss Analysis of GaN Devices in an Isolated Bidirectional DC-DC Converter," *Proc. IEEE Workshop on Wide Bandgap Power Devices and Applications*, 2015, pp. 201–205.

[27] F. Pulsinelli *et al*., "Power Losses Distribution in SiC Inverter Based Electric Motor Drives," *IEEE Trans. Ind. Appl*, vol. 55, no. 6, pp. 7843–7853, 2019.

BIOGRAPHY OF AUTHOR

Pekik Argo Dahono received bachelor degree from the Institute of Technology Bandung, Indonesia, in 1985, Master of Engineering and Doctor of Engineering degrees from the Tokyo Institute of Technology, Japan, in 1992 and 1995, respectively, all in electrical engineering. At present, he is a professor in the School of Electrical Engineering and Informatics, Institute of Technology Bandung. He has interests in power electronics, power quality, and industrial power systems. He is a cofounder of Indonesia Power Quality Initiatives and Indonesia Smart Grid Initiatives. He has published more than 100 international and national papers. He is recipient of ASEAN Engineer Outstanding Achievement Award in 2006 and 2014. He is registered as a professional engineer in Indonesia and ASEAN. He is a senior member of IEEE. He was a Hitachi Post-Doctoral Fellow in Tokyo Institute of Technology, Japan, in 1997-1998. He was a visiting professor in Tokyo Institute of Technology, Science University of Tokyo, and Tokyo Denki University, in 1998, 2001, and 2004, respectively. He was also a visiting professor in University of Toulouse, France, in 2008.